JOURNAL OF SPACECRAFT AND ROCKETS
Vol. 43, No. 6, November–December 2006

Application of Solar Electric Propulsion to a Comet Surface Sample Return Mission

Byoungsam Woo* and Victoria L. Coverstone†
University of Illinois at Urbana–Champaign, Urbana, Illinois 61801
and
Michael Cupples‡
Science Applications International Corporation, Huntsville, Alabama 35806

DOI: 10.2514/1.23371

Current NASA solar electric propulsion technology application readiness and NASA's evolutionary xenon thruster-based propulsion systems are compared for a comet surface sample return mission to Tempel 1. Mission and systems analyses are conducted over a range of array power for each propulsion system and for two medium-class launch vehicles. Engine configurations investigated for NASA solar electric propulsion technology application readiness included five operational engines with one spare and six operational engines with one spare. The NASA evolutionary xenon thruster configuration investigated included two operational engines plus one spare, with performance estimated for two different throttling modes. Figures of merit for this comparison include solar electric propulsion dry mass, average engine throughput, and net nonpropulsion payload returned to Earth. For the comet surface sample return mission, the NASA evolutionary xenon thruster system outperforms the NASA solar electric propulsion technology application readiness system with the advantage of lighter dry mass and simpler hardware implementation.

Introduction

WITH the success of the Deep Space 1 mission [1,2], the potential of solar electric propulsion (SEP) systems was clearly demonstrated, making SEP a strong candidate for various interplanetary missions. The long-duration high-efficiency operation of SEP allows for new ways to explore the inner and outer solar system and enables missions that can be difficult and expensive to achieve with chemical propulsion systems. This study provides a parametric comparison of two SEP systems based on a typical comet surface sample return (CSSR) mission [3,4]. The first SEP system is based on the NASA solar electric propulsion technology application readiness (NSTAR) system, considered the benchmark propulsion system for this study. The NSTAR thruster system chosen for this analysis is the one planned for NASA's discovery mission Dawn. NASA has undertaken an ion propulsion system development program to create a new ion propulsion system based on NASA's evolutionary xenon thruster (NEXT) [5]. The second SEP system is based on the NEXT system being developed through the NEXT Generation Electric Propulsion Technology Area Office under the In-Space Propulsion Technology Projects at the Marshall Space Flight Center [6]. The NEXT-based propulsion system is designed to have a higher maximum design power than NSTAR along with advances in both the power processing and propellant management.

Previous studies have investigated the application of NEXT to flagship-class missions such as Titan Explorer and Neptune Orbiter [7–9]. A recent study provides a summary of current applications of the NEXT thruster to deep space missions [7]. The study herein compares the NSTAR- and NEXT-based propulsion systems in the context of a New Frontiers-class mission.§ A comet surface sample return mission to Tempel 1 is chosen because it is challenging and could probably be performed within the New Frontiers cost cap.

The primary figures of merit employed to compare the NEXT and NSTAR systems are nonpropulsive system mass returned to Earth after completing all mission requirements, average engine throughput, and SEP system dry mass. The parametric study performed investigated the efficiency of the propulsion systems over 1) a range of power levels, 2) a number of operational thrusters, and 3) thruster throttling modes. For the NSTAR-based system, cases investigated included five operational thrusters with one spare (NSTAR $5+1$ case) and six operational thrusters with one spare (NSTAR $6+1$ case). This variation in thruster number allows a determination of best performance based on a variation of the array power measured at 1 AU from the sun. For the NEXT thrusters, two throttling modes are explored. The throttling modes are modeled by polynomial fitting of throttle data from previous tests [10]. In this study, the polynomials that model the high-thrust throttling and high-I_{sp} throttling modes are selected for trajectory analysis and optimization. The high-thrust throttling or high-I_{sp} throttling are representations of operational throttling modes of the NEXT thruster rather than an actual difference of hardware. During a specific mission, the NEXT thruster can operate at different modes, but the throttling mode is set to one of the high-thrust throttling or high-I_{sp} throttling modes during a mission for the trajectory optimization because the trajectory optimization tool used in this study does not allow variations of throttling mode during a mission. Therefore, two different NSTAR systems and two different NEXT throttling modes are compared: NSTAR $5+1$, NSTAR $6+1$, NEXT high-thrust throttling mode, and NEXT high-I_{sp} throttling mode. Two medium-class launch vehicles, the Delta IV 4040 and the Delta IV 4240, are considered for each case.

Mission Descriptions

Tempel 1 is the target of the CSSR mission in this study. Figure 1 depicts orbits of the Earth and Tempel 1. The primary objective of the

Presented as Paper 3804 at the 40th AIAA/ASME/SAE/ASEE Joint Propulsion Conference and Exhibit, Fort Lauderdale Florida, 11–14 July 2004; received 22 February 2006; revision received 10 May 2006; accepted for publication 11 May 2006.

*Postdoctoral Researcher, Department of Aerospace Engineering, 104 S. Wright Street. Member AIAA

†Professor, Department of Aerospace Engineering, 104 S. Wright Street. Associate Fellow AIAA.

‡Lead Systems Engineer, In-Space Technology Assessment.

§Data available online at http://centauri.larc.nasa.gov/newfrontiers/ [cited July 2004].

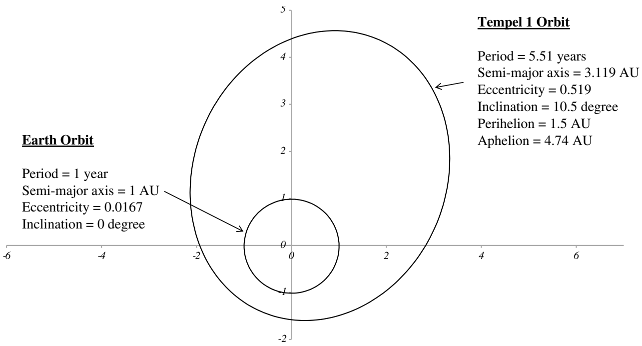

Fig. 1 Earth and Tempel 1 orbit depiction.

mission is for the spacecraft to rendezvous with Tempel 1, collect a sample, and return the sample to Earth. A launch vehicle places the spacecraft on an optimal Earth escape trajectory, and the SEP system provides an optimal transfer to rendezvous with Tempel 1 and also provides the return propulsion for an arrival to Earth with constrained arrival entry interface velocity. Table 1 shows the assumed characteristics in the CSSR mission.

To analyze the performance of different SEP systems, the total delivered mass of SEP systems (SEP delivered mass) are compared. The SEP delivered mass consists of two mass components: 1) 210 kg of science payload that includes the sampling system, the sample return system, and minimal science instruments (e.g., cameras) and 2) the nonpropulsive spacecraft mass (e.g., subsystems including the navigation, attitude control, communications, command and control, structure, power, and thermal systems).

Systems Assumptions

The launch vehicles chosen for this investigation are the Delta IV 4040 and the Delta IV 4240.‖ These are Delta medium-class launch vehicles and are suited for minimizing cost in New Frontiers-class missions. Figure 2 illustrates the launch vehicle models as included in the trajectory optimization process. The injected mass in Fig. 2 is the launch vehicle payload capability as a function of C_3. The launch vehicle contingency is assumed as 0% in Fig. 2 and also in the trajectory optimization process. Detailed SEP system models are developed and used to perform the parametric comparison. The system models for each SEP system include power and power conversion/distribution, thrusters, power processing unit (PPU), propellant management and tank, structures, and thermal control (radiators and loop heat pipe). SEP system models are either physics-based or derived using scaling laws from actual spacecraft data. For example, the SEP system structure model is derived from a spacecraft database including Cassini, Galileo, Mars Global Surveyor, Near, Odyssey, and Mars Climate Orbiter. The SEP configurations are shown in Figs. 3 and 4. Several other system assumptions including the Xe propellant contingency, the system's dry mass contingency, and redundancy are also shown in Figs. 3 and 4. The duty cycle of the propulsion system is assumed as 90% in the trajectory optimization process.

The solar array is assumed as the only source of propulsion power for the system (other than battery power during solar array deployment). The array power model employed in the trajectory optimization is based on multijunction GeAs array technology [11] with an Ultraflex lightweight array structure [12]. The performance of this solar array technology is slightly below $1/r^2$ solar insolation as shown in Fig. 5. In Fig. 5, the array power at 1 AU from the sun (P_0) is set to 13 kW.

The Ultraflex array concept is also depicted in Fig. 5. In this study, we added 2% to the array area for degradation contingency requirements. Also, 5% of the baseline array is added to the beginning-of-life power as the power contingency. The house-keeping power of 0.25 kW is included in the power system design.

‖Data available online at http://elvperf.ksc.nasa.gov [cited July 2004].

Table 1 Mission specifications

Parameter	Specification
Target	Tempel 1
Launch year	2013
Launch type	Optimized C_3
Stay time at Tempel 1	60 days
Science payload	210 kg
Sampling system (mass dropped at Tempel 1)	140 kg
Sample return system	60 kg
Cameras	10 kg
Earth return	Hyperbolic excess velocity <13 km/s

Trajectory Optimization

Trajectory optimization with variable thrust and thrust direction has been previously investigated [13–15]. Solutions typically require the optimization of a number of parameters. For the cases investigated in this study, the final delivered mass to Earth is maximized by optimizing 16 parameters: the launch date, the comet rendezvous date, the time of flight, the launch energy, the B-plane angle, the thrust switching function, and the Lagrange multipliers

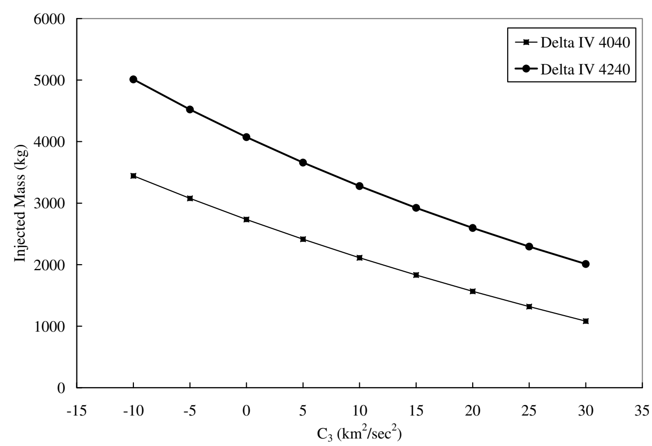

Fig. 2 Launch vehicle performance model.

- 5 engines + 1 spare
- 6 engines + 1 spare
- PPU max. power = 2.56 kW
- PPU min. power = 0.60 kW
- Propellant contingency = 10% of Xe deterministic
- Dry mass contingency = 30% of dry mass
- 1 spare includes thruster, PPU and propellant distribution string

Fig. 3 Major NSTAR thruster system assumptions.

- 2 engines + 1 spare
- PPU max. power = 7.25 kW
- PPU min. power = 0.62 kW
- Propellant contingency = 8.6% of Xe deterministic
- Dry mass contingency = 30% of dry mass
- 1 spare includes thruster, PPU and propellant distribution string

Fig. 4 Major NEXT thruster system assumptions.

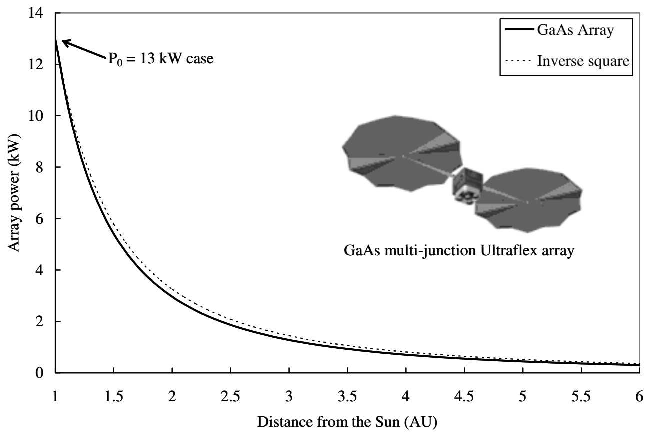

Fig. 5 Solar array system model.

about primer vectors at Earth departure and departure from the comet. The trajectory optimization is performed using the solar electric propulsion trajectory optimization program (SEPTOP) [16]. SEPTOP is a two-body sun-centered, low-thrust trajectory optimization program for preliminary mission feasibility studies that provides relatively accurate performance estimates. The program determines a numerical solution to a two-point-boundary-value problem that satisfies intermediate boundary constraints. In SEPTOP, the user estimates initial values of the optimizing parameters and then uses a shooting method to integrate the trajectory from an initial time to final time. SEPTOP computes an error at the final time and uses it to correct the estimate of the initial values. This process is repeated until the error becomes smaller than the prescribed tolerance. The required mission/system input assumptions are nominal Earth departure year, array power at 1 AU, maximum/minimum power into PPU, and launch vehicle model. SEPTOP can model variable thrust and mass flow rate as a function of power into the PPU. The power generated from a solar array is modeled as a function of the spacecraft's distance from the sun (Fig. 5). Therefore, the SEP thruster and solar array models are also required as inputs. Earth arrival is constrained with the entry interface velocity equal or less than 13 km/s [17].

The trajectory optimization requires an experienced initial value estimation because the parameter space of the CSSR mission is nonconvex with 16 parameters to search [18]. The trajectory from SEPTOP is a local optimal solution and there exist multiple local optimal solutions. In this study, the best performing trajectory is selected among the generated local optimal solutions.

Performance Comparison

Figure 6 shows a typical trajectory used for the CSSR mission to Tempel 1. The trajectory is generated with NEXT high-thrust mode and P_0 of 12.4 kW. This trajectory, however, shares the following salient characteristics with all the other trajectories of this study: 1) the Tempel 1 rendezvous happens near October 2016, 2) the total mission time is roughly eight years, and 3) the Earth arrival entry interface velocity is 13 km/s.

Variation in Performance Because of Launch Vehicle and SEP Model

As shown in Fig. 2, the launch capacity (C_3 + injected mass) of the Delta IV 4240 is larger than that of the Delta IV 4040. Therefore, the trajectories generated with Delta IV 4240 are likely to deliver more mass back to Earth or deliver the same mass with less array power than the trajectories with Delta IV 4040. Figures 7 and 8 compare the performances of the NSTAR and NEXT models with the Delta IV 4040 and the Delta IV 4240 launch vehicles. Again, the SEP delivered mass in Figs. 7 and 8 is total delivered mass of different SEP systems. Figure 7 shows the result of varying the number of operational propulsion strings (thruster, PPU, and propellant distribution and control) of the NSTAR propulsion system. The minimum P_0s that deliver the science payload of 210 kg

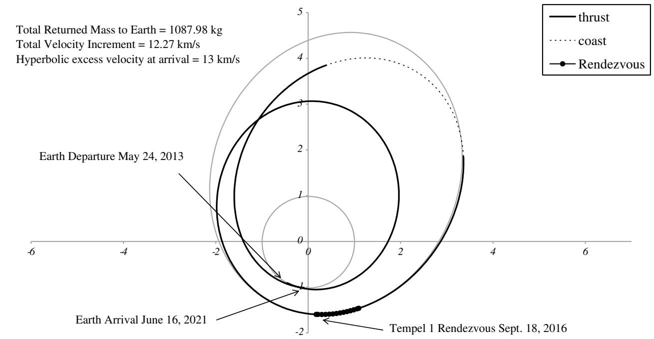

Fig. 6 Typical CSSR mission trajectory: NEXT high-thrust 2 + 1 engine, $P_0 = 12.4$ kW, and Delta IV 4240.

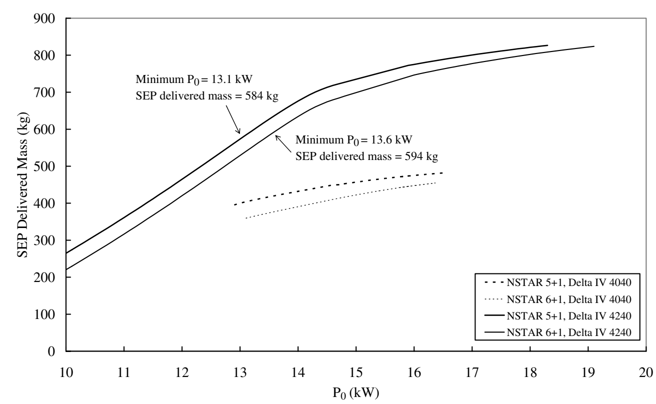

Fig. 7 NSTAR SEP delivered mass over a range of array power and engine configurations.

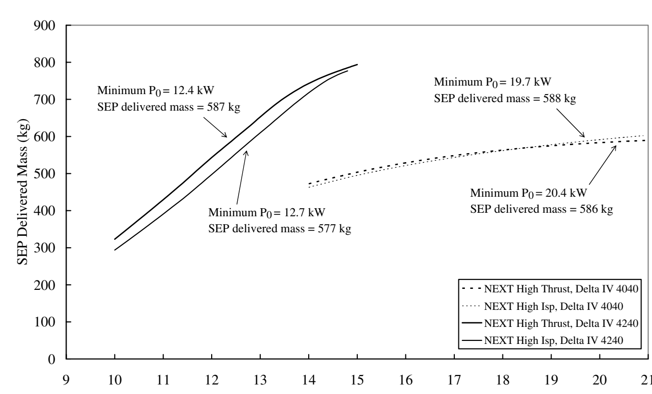

Fig. 8 NEXT SEP delivered mass over a range of array power and throttling modes.

are marked in Fig. 7. Note that there is no optimal trajectory found that could deliver the science payload for the Delta IV 4040 with the NSTAR systems. The Delta IV 4240, however, with the NSTAR 5 + 1 system delivers the science payload for a P_0 of 13.1 kW, and the NSTAR 6 + 1 system delivers the science payload for a P_0 of 13.6 kW. Given that six thrusters at a maximum power of 2.56 kW each implies a maximum power usage of over 15.3 kW at 1 AU, the 6 + 1 configuration allows the system to use all of the available array power of 13.6 kW (minus housekeeping) at 1 AU. Five thrusters at a maximum power of 2.56 kW each provides a maximum power usage of less than 12.8 kW at 1 AU, implying that the 5 + 1 configuration does not permit the full array power of 13.1 kW to be used at 1 AU. Yet as Fig. 8 shows, the NSTAR 5 + 1 configuration performed modestly better than the 6 + 1 configuration due to an overpowering increase in dry mass for the 6 + 1 case.

Figure 8 shows the performance of the NEXT thruster with two different operating modes. The number of operating thrusters is two with one spare each for both modes. In Fig. 8, the NEXT thruster at high-thrust mode delivers the science payload for a P_0 of 20.4 kW on

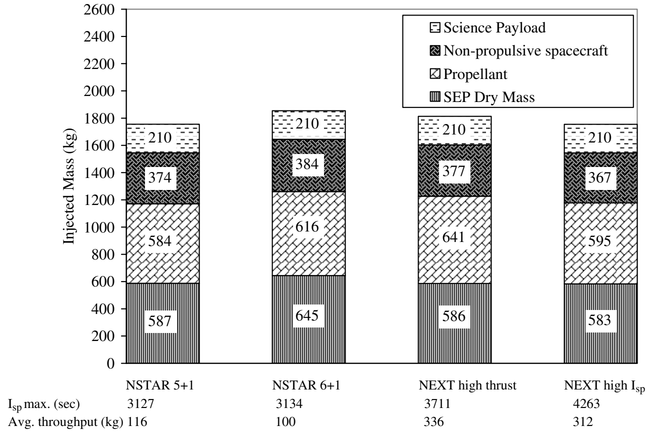

Fig. 9 Comparison of mission stack mass for NEXT and NSTAR using Delta IV 4240.

a Delta IV 4040 or at a P_0 of 12.4 kW on a Delta IV 4240. The minimum P_0s that deliver the science payload are also marked in Fig. 8. The NEXT thruster at high-I_{sp} mode delivers the science payload at a P_0 of 19.7 kW on a Delta IV 4040 or at a P_0 of 12.7 kW on a Delta IV 4240. In summary, the NEXT thruster performed better than NSTAR over the range of investigated power, with NEXT providing roughly 80 kg more SEP delivered mass over NSTAR for a P_0 of 13 kW on a Delta IV 4240.

Performance at Minimum Array Power for Science Payload Delivery

A comparison of NSTAR and NEXT is performed at the minimum P_0s that deliver the 210 kg of science payload. We compared the results only for the Delta IV 4240 launch vehicle because there were no trajectories found with Delta IV 4040 for the NSTAR combinations that deliver the science payload. An overall stack mass comparison is shown in Fig. 9. The NSTAR $5 + 1$ case provides 584 kg of SEP delivered mass with a P_0 of 13.1 kW, as compared with 594 kg of SEP delivered mass for the NSTAR $6 + 1$ case with a P_0 of 13.6 kW. The NEXT case using the high-thrust throttling mode provides 587 kg of SEP delivered mass with a P_0 of 12.4 kW, and the case using the high-I_{sp} throttling mode provides 577 kg of SEP delivered mass with a P_0 of 12.7 kW. Thus, for the Tempel 1 CSSR mission, both NEXT cases show improvement over NSTAR in payload delivery capability because NEXT cases deliver the science payload with smaller P_0. Also this NEXT payload delivery is realized with a $2 + 1$ engine configuration that may imply significant cost and complexity benefits over the $5 + 1$ or $6 + 1$ NSTAR configuration.

In addition to the SEP delivered mass and the science payload capability of each case, Fig. 9 also indicates the SEP dry mass, the propellant mass for the SEP system, the maximum I_{sp}, and the average engine throughput. In this study, the design requirement for the average engine throughput is less than 150 kg for NSTAR systems and less than 300 kg for NEXT system. Because the NEXT system is undergoing tests, the current throughput requirement for the NEXT system is set to be very conservative. In Fig. 9, the average engine throughputs for all NSTAR cases are well below the NSTAR engine design requirements of 150 kg. For the NEXT high-I_{sp} case, the average engine throughput is about 4% over the design throughput requirement. By considering the level of maturity of the NEXT hardware, the excess of 4% could be considered as an appropriate performance of the system in the mission although the NEXT high-thrust case would not be considered as an appropriate performance for the CSSR mission because it exceeds the throughput design requirement by 12% (36 kg).

The selection of the thruster system for a mission needs to consider many factors. For the CSSR mission considered in this study, the NEXT system outperforms the NSTAR system in a number of ways. First, the NEXT system can perform the mission on a smaller launch vehicle (Delta IV 4040) than the NSTAR system. For the same slightly larger launch vehicle (Delta 4240), the NEXT system can perform the mission with modestly less power requirements than the NSTAR system. Second, for the Delta IV 4240, the NEXT system is modestly less massive than NSTAR system and requires only two operational thrusters rather than the five operational thrusters required for the NSTAR system. In this study, the NSTAR systems and NEXT system in high-I_{sp} mode satisfy the throughput requirement whereas the NEXT system in high-thrust mode does not.

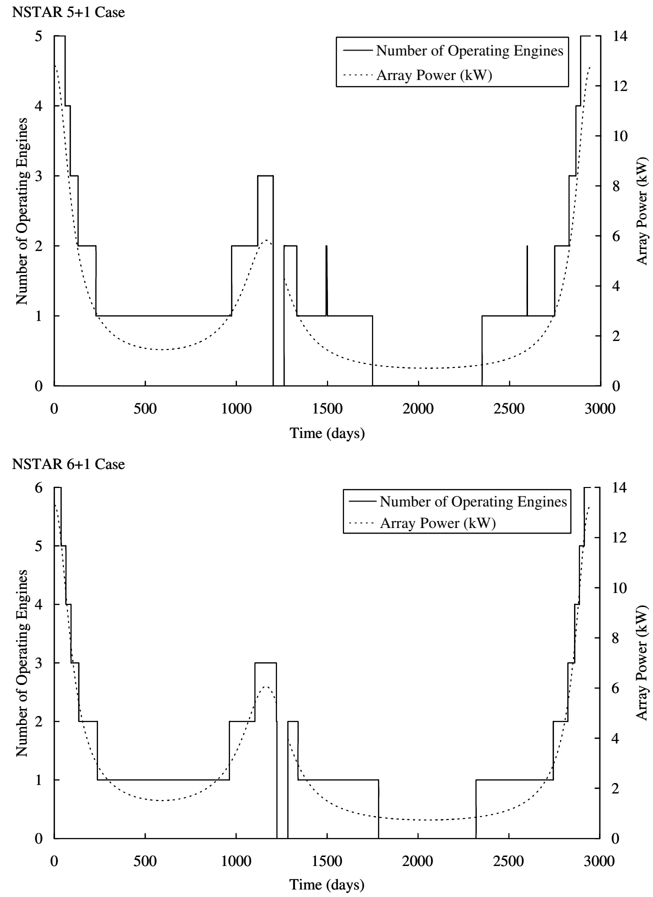

Fig. 10 NSTAR engine operation history.

Thrust Histories at the Minimum Array Power to Deliver the Science Payload

Figures 10 and 11 show engine on–off time histories with their corresponding SEP system power levels for each of the four cases identified in Fig. 9. For each case, the array power level is the minimum P_0 that delivers the science payload, and the transfer time is approximately eight years. Figures 10 and 11 provide power profiles as a function of mission time and facilitate a determination of how well the SEP system is using the power during the course of the mission.

The NSTAR $5 + 1$ and $6 + 1$ engine configurations are compared in Fig. 10. During most of the mission, three or less thrusters are required, and for only a short time during the beginning and the end of the mission, five or six thrusters are in operation. Thus, Fig. 10 provides some corroborating evidence for the better performance seen earlier for the $5 + 1$ configuration, given that for the $6 + 1$ configuration the very small increase in overall power usage improvement is overcame by the relatively large increase in system dry mass. In addition, given that five thrusters (or six thrusters, depending on the case) are needed for only a short time during the beginning of the transfer, it might be possible to eliminate the spare thruster (along with the related mass) and operate without a spare during the first part of the mission. This operation would, however, significantly increase the mission risk. A similar argument could be made for the NEXT $2 + 1$ configuration shown in Fig. 11, but mission risk would increase more in this case.

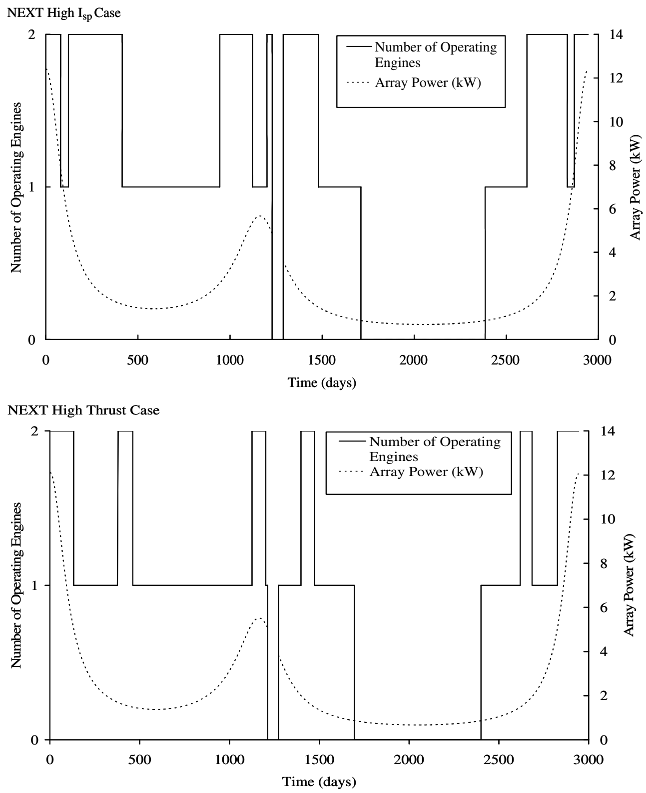

Fig. 11 NEXT engine operation history.

A comparison of the NEXT high-thrust with the NEXT high-I_{sp} throttling mode is provided in Fig. 11. The NEXT high-I_{sp} case shows more usage of two engines than the NEXT high-thrust case, and this contributes to the performance difference between the NEXT high-I_{sp} and the NEXT high-thrust cases. To understand the difference in operation between the thrusters, it must be understood that for a given power level an engine operating in the high-thrust throttling mode generates a higher thrust level than the same engine operating in the high-I_{sp} throttling mode. It is also true that for a given power level (where the power level is low enough that either one or two engines can operate simultaneously) the thrust generated by two engines equally dividing the total available power can be more than the thrust generated by one engine alone operating at the same total available power. Therefore, throughout the mission, the trajectory optimizer finds that it can be more beneficial to operate two engines at higher thrust during a part of the trajectory than to operate one engine at higher power. For the high-thrust case, the higher thrust provided by the high-thrust throttling mode is adequate, and thus the optimizer finds that throttling to two engines is not required. The history of the number of operating engines also explains how the NEXT high-thrust case accomplishes the same mission with slightly less P_0 (0.3 kW) than the NEXT high-I_{sp} case. The high-thrust case more efficiently uses the two engines, and this reduces the need for power. However, with its relatively low I_{sp}, the NEXT high-thrust case consumes significantly more (45 kg) propellant than the NEXT high-I_{sp} case.

In general, the NSTAR and NEXT engines can operate at high-AU (more than 3 AU from the Sun) because the minimum thruster power level for each thruster is 0.60 kW and 0.62 kW, respectively. Figures 6, 10, and 11 show this high-AU operation for the mission phase between 1500 and 2500 days of the mission time. The ability of a high-AU operation provides significant flexibility in trajectory optimization especially for the CSSR mission given the need for active trajectory control near the target comet.

Summary and Conclusions

Four SEP systems based on NSTAR and NEXT models were compared for a comet surface sample return mission to Tempel 1. Two launch vehicles were chosen for the trajectory analysis. There was no optimal trajectory found that delivered the science payload for the Delta IV 4040 with the NSTAR systems whereas the Delta 4240 could deliver the science payload with both the NSTAR and the NEXT systems. A range of array power was investigated, and the minimum array power to deliver the science payload was found for each propulsion system. Engine configurations investigated for the NSTAR model included $5 + 1$ and $6 + 1$ engines, and the NEXT configuration included only a $2 + 1$ case. For NSTAR, the $5 + 1$ engine configuration provided a modest performance advantage over the $6 + 1$ configuration. The NEXT $2 + 1$ configurations were compared with the NSTAR systems, with a small performance advantage going to the NEXT thruster. It should be noted, however, that the NEXT $2 + 1$ SEP configuration is lighter in dry mass and less complex in hardware implementation, resulting in a significantly less costly SEP vehicle than the NSTAR SEP vehicle. In both the NEXT and the NSTAR cases, power and engine operation time history showed smooth variation in thruster on–off sequences following the available power to the SEP system. Because of the rather low minimum throttle points of 0.60 kW and 0.62 kW for NSTAR and NEXT, respectively, the thrusters performed effectively at the higher AU points of the trajectories. It was found for NSTAR that five or six thrusters are needed for only a short time during the beginning and the end of the transfer. Thus, it might be possible to eliminate the spare thruster (along with the related mass) for the mission, but the mission risk would increase. A similar argument could be made for the NEXT $2 + 1$ configuration, but mission risk would increase more than in the NSTAR cases. Finally, engine throughput for NSTAR and NEXT are within the accepted design limits of 150 kg for NSTAR and 300 kg for NEXT for all cases investigated except for the NEXT high-thrust throttling case.

Acknowledgements

The work described in this paper was performed by Science Applications International Corporation under contract with the NASA Marshall Space Flight Center (MSFC). Special thanks go to the NASA MSFC In-Space Propulsion Technology Investment Projects and to the NASA MSFC Next Generation Electric Propulsion Technology Area for providing direction to this work.

References

[1] Rayman, M. D., and Williams, S. N., “Design of the First Interplanetary Solar Electric Propulsion Mission,” *Journal of Spacecraft and Rockets*, Vol. 39, No. 4, 2002, pp. 589–595.

[2] Rayman, M. D., Chadbourne, P. A., Culwell, J. S., and Williams, S. N., “Mission Design for Deep Space 1: A Low-Thrust Technology Validation Mission,” International Academy of Astronautics, Paper L98-0502, April 1998.

[3] Tan, G. H., and Sims, J. A., “Mission Design for the Deep Space 4/Champollion Comet Sample Return Mission,” *American Astronautical Society/AIAA Space Flight Mechanics Meeting*, American Astronautical Society Paper 98-187, Feb. 1998.

[4] Sims, J. A., “Trajectories to Comets Using Solar Electric Propulsion,” *American Astronautical Society/AIAA Space Flight Mechanics Meeting*, American Astronautical Society Paper 2000-134, Jan. 2000.

[5] Patterson, M. J., Foster, J. E., Haag, T. W., and Soulas, G. C., “Next: NASA’S Evolutionary Xenon Thruster Development Status,” *Proceedings of the 39th Joint Propulsion Conference*, AIAA Paper 2003-4862, July 2003.

[6] Johnson, C. L., Alexander, L., Baggett, R. M., Bonometti, J. A., Herrmann, M., James, B. F., and Montgomery, S. E., “NASA’s In-Space Propulsion Technology Program: Overview and Status,” *Proceedings of the 52nd Joint Army-Navy-NASA-Air Force (JANNAF) Propulsion Meeting*, JANNAF Paper 2004-0031, May 2004.

[7] Cupples, M. L., Green, S. H., and Coverstone, V., “Factors Influencing Solar Electric Payload Delivery to Outer Planet Missions,” *American Astronautical Society/AIAA Space Flight Mechanics Conference*, American Astronautical Society Paper 03-123, Feb. 2003.

[8] Cupples, M., Green, S., Donahue, B., and Coverstone, V., “Solar Electric and Chemical Propulsion for a Titan Mission,” *Proceedings of the 39th Joint Propulsion Conference*, AIAA Paper 2003-4728, July 2003.

[9] Byoungsam, W., Coverstone, V., Hartmann, J., and Cupples, M., "Trajectory and Systems Analysis for Outer Planet Solar Electric Propulsion Missions," *Journal of Spacecraft and Rockets*, Vol. 42, No. 3, 2005, pp. 510–516.

[10] Oh, D., Sims, J., Benson, S., Gefert, L., Witzberger, K., and Cupples, M., "Deep Space Applications of the NEXT Thruster," AIAA Paper 2004-3806, July 2004.

[11] Kerslake, T., "Photovoltaic Array Performance during an Earth-to-Jupiter Heliocentric Transfer," NASA Glenn Research Center Rept. PS-496, Aug. 2000.

[12] Able Engineering Company, Inc., *Ultra Flex Solar Array* [online database], http://www.aec-able.com/arrays/Resources/Ultraflex%20PDS.pdf [cited July 2004].

[13] Sauer, C. G., "Optimization of Multiple Target Electric Propulsion Trajectories," *AIAA 11th Aerospace Sciences Meeting*, AIAA Paper 73-205, Jan. 1973.

[14] Melbourne, W. G., Richardson, D. E., and Sauer, C. G., "Interplanetary Trajectory Optimization with Power-Limited Propulsion Systems," Jet Propulsion Laboratory, California Institute of Technology, TR 32-173, Pasadena, CA, 1962.

[15] Williams, S. N., and Coverstone, V. L., "Mars Missions Using Solar Electric Propulsion," *Journal of Spacecraft and Rockets*, Vol. 37, No. 1, 2000, pp. 71–77.

[16] Williams, S. N., "An Introduction to the Use of VARITOP: A Ggeneral Purpose Low-Thrust Trajectory Optimization Program," Jet Propulsion Laboratory, California Institute of Technology, JPL D-11475, Pasadena, CA, 1994.

[17] Dachwald, B., Seboldt, W., and Richter, L., "Multiple Rendezvous and Sample Return Missions to Near-Earth Objects Using Solar Sailcraft," *Proceedings of the 5th IAA Conference on Low-Cost Planetary Missions*, SP-542, ESA Publications Div., Paris, 2003, pp. 351–358.

[18] Woo, B., Converstone, V. L., and Cupples, M., "Low-Thrust Trajectory Optimization Procedure for Gravity-Assist, Outer-Planet Missions," *Journal of Spacecraft and Rockets*, Vol. 43, No. 1, 2006, pp. 121–129.

J. Martin
Associate Editor